An Enhanced Ray-Shooting Approach to Force-Closure Problems

Yu Zheng
e-mail: yuzheng007@sjtu.edu.cn

Wen-Han Qian
e-mail: whqian@sh163.net

Robotics Institute,
Shanghai Jiao Tong University,
Shanghai 200030, China

Force-closure is a fundamental topic in grasping research. Relevant problems include force-closure test, quality evaluation, and grasp planning. Implementing the well-known force-closure condition that the origin of the wrench space lies in the interior of the convex hull of primitive wrenches, Liu presented a ray-shooting approach to force-closure test. Because of its high efficiency in 3D work space and no limitation on the contact number of a grasp, this approach is advanced. Achieving some new results of convex analysis, this paper enhances the above approach in three aspects. (a) The exactness is completed. In order to avoid trouble or mistakes, the dimension of the convex hull of primitive wrenches is taken into account, which is always ignored until now. (b) The efficiency is increased. A shortcut which skips some steps of the original force-closure test is found. (c) The scope is extended. Our simplified ray-shooting approach yields a grasp stability index suitable for grasp planning. Numerical examples in fixturing and grasping show the enhancement superiority. [DOI: 10.1115/1.2336259]

Keywords: force-closure, grasp planning, multifingered robot hand, ray-shooting approach

1 Introduction

Multifingered robotic grasping has been ardently studied since the pioneer work of Salisbury and Roth [1]. Force-closure is a fundamental topic in grasping research. This property means the capability of a grasp to equilibrate any external wrench and to restrain any motion on the grasped object. It is a prerequisite to stable grasping. Force-closure problems mainly include:

- Force-closure test: given contact positions on an object, determine if the grasp is force-closure.
- Grasp quality evaluation: given contact positions on an object, evaluate the closure quality of the grasp by a performance index.
- Optimal grasp planning: given an object, determine the contact positions to construct a force-closure grasp with optimal performance quality.

These problems can be discussed in the *wrench space* [1–5], the *contact force space*, [6–10], or their dual spaces [10–13]. The wrench space and its dual space are 6D vector spaces, while the dimensions of the contact force space and its dual space are both $m_0+3m_f+4m_s$, where m_0, m_f, and m_s are numbers of frictionless point contacts, frictional point contacts, and soft finger contacts, respectively.

1.1 Related Work. Investigation in the wrench space tells that a grasp is force-closure if and only if the primitive wrenches positively span the entire wrench space [1], or equivalently, the origin of the wrench space is an interior point of the convex hull of the primitive wrenches [2]. By implementing this condition, after the 2D test [3] Liu [4] presented a ray-shooting based algorithm for 3D. Zhu et al. [5] proposed a generally applicable algorithm without linearizing the friction cones. In the contact force space, Murray et al. [6] revealed that a grasp is force-closure if and only if the grasp matrix is surjective and there is a strictly internal force. Various forms of this condition can be found in Refs. [7–10]. Zuo and Qian [7] extended the condition to soft multifingered grasps. Following Buss et al. [8], Han et al. [9] formulated force-closure test as a convex optimization problem involving linear matrix inequalities. Bicchi [10] took account of the kinematics of the grasping mechanism. Recently, Zheng and Qian [13] generalized the method of form-closure analysis [10–12] to force-closure by the duality between the infinitesimal motion and the wrench.

As a higher topic than qualitative test, quantitative evaluation indicates the goodness of various grasps. Optimal grasp planning cannot proceed without it. Li and Sastry [14] presented three quality measures: the smallest singular value and the volume of the grasp matrix as well as a task-oriented measure. Zuo and Qian [7], Buss et al. [8], evaluated the stability of a grasp by its extent to satisfy the friction constraints. Zheng and Qian [13] explored the tolerance of force-closure grasps to some grasping uncertainties. Kirkpatrick et al. [15], Ferrari and Canny [16] assessed the "efficiency" by the radius of the largest ball centered at the origin of the wrench space, contained in the convex hull of the primitive wrenches. Using the Q distance, Zhu and Wang [17] made it possible to compute the measure of efficiency for the first time. Other quality measures were proposed by Varma and Tasch [18], Xiong and Xiong [19], Salunkhe et al. [20].

An early stage of optimal grasp planning research focused on synthesizing force-closure grasps on simple objects with limited contacts. On polygonal objects, Nguyen [21] computed independent regions for two frictional or four frictionless point contacts to achieve a force-closure grasp. Markenscoff and Papadimitriou [22] proposed an analytic method for calculating the optimum grip. Park and Starr [23] built a 3-finger grasp, while Tung and Kak [24] fast constructed a 2-finger one. On irregular 2D and 3D objects, Chen and Burdick [25] considered 2-finger antipodal point grasps. Li et al. [26] developed a geometrical algorithm for computing 3-finger force-closure grasps. Ponce and co-workers [27–29] extended Nguyen's [21] idea to 2-finger, 3-finger, and 4-finger force-closure grasps on 2D curved, polygonal, and polyhedral objects, respectively. In the recent years, limitation on the contact number has been eliminated. Liu [30] calculated n-finger grasps on polygons. Ding et al. [31] considered 3D n-finger grasps

Contributed by the Manufacturing Engineering Division of ASME for publication in the Journal of Manufacturing Science and Engineering. Manuscript received August 31, 2005; final manuscript received June 24, 2006. Review conducted by G. Wiens.

whose k fingers have been located in advance. Based on the Q distance, Zhu and Wang [17] planned optimal grasps on 3D objects with curved surfaces. With the ray-shooting based algorithm [4], Liu et al. [32] sought force-closure grasps on objects in the discrete domain. In addition, the algorithm for fixture design can be applied to grasp planning as well [33].

1.2 Our Work. In the previous work, we are especially interested in the ray-shooting approach [4]. Since Mishra et al. [2] proposed the force-closure condition, no algorithm implemented it on 3D grasps during the succeeding twelve years until Liu put forward the ray-shooting based algorithm [4]. Up to the present, it is still the fastest way to force-closure test and frequently used in grasp planning as well as fixture design [31–33]. After repeatedly studying his work, we first found a shortcut to simplify its application to force-closure test [34]. Second, we discover that, although the test algorithm is valid in most cases, it may commit errors because the *dimension* of the convex hull of primitive wrenches is ignored. When the convex hull is below 6D, the linear programming (LP) formulation for solving the ray-shooting problem will be unbounded, or the origin will be mistaken for an interior point of the convex hull. This motivates us to investigate the dimension and the relative interior of a convex set. According to the dimensions and the relative positions to the origin, we classify the convex hulls into four categories. A grasp is force-closure if and only if the convex hull is 6D and contains the origin as a relative interior point, so that the origin lies in its interior. The former condition is equivalent to that the grasp matrix has full row rank and a certain linear system is consistent. The latter can be determined by the simplified ray-shooting approach. The consistency of the linear system ensures that our LP formulation is bounded and always has solution. Third, the simplified ray-shooting approach turns out a grasp *stability* index, which is relevant to the inclination angles of contact forces. It has different meaning from the *quality* indices [15–17], which reflect the resultant wrenches generated by a grasp. Compared with other formulations of grasp stability [7,8], ours is easier to compute. Furthermore, the original ray-shooting approach [4,32] does not yield such an index, so the index is applied to optimal grasp planning of arbitrary 3D objects for the first time. Needless to say, all the above start from Liu's trailblazing work [4]. In addition, for use in derivation, we deduce a number of theorems of convex analysis. Some of them are brand new.

2 Preliminaries

Our work is based on the following assumptions:

1. The fingers and the grasped object are rigid bodies. Like Refs. [1–34], we do not consider their compliance and contact region deformation as Refs. [35–37], etc. All contacts are point-to-point hard contacts.
2. Each finger contacts the object at a regular point, where $\mathbf{n}_i$, $\mathbf{o}_i$, and $\mathbf{t}_i$ are well defined.
3. The finger number $m \geqslant 3$, which is a prerequisite for achieving 3D force-closure.

Consider an m-finger robot hand grasping a 3D object, fixed with a right-handed coordinate frame. The contact force $\mathbf{f}_i$ at contact i can be expressed in the local coordinate frame $\{\mathbf{n}_i, \mathbf{o}_i, \mathbf{t}_i\}$ by

$$\mathbf{f}_i = [f_{in}\ f_{io}\ f_{it}]^T \tag{1}$$

To avoid separation and slippage at contact, $\mathbf{f}_i$ must satisfy

$$f_{in} \geqslant 0, \quad f_{io}^2 + f_{it}^2 \leqslant \mu^2 f_{in}^2$$

The above nonlinear contact constraint defines a circular cone called a friction cone. For simplicity, we substitute an n-sided polyhedral cone for it ($n \geqslant 3$ since the friction cone is 3D), as shown in Fig. 1. The side edges are expressed in the frame $\{\mathbf{n}_i, \mathbf{o}_i, \mathbf{t}_i\}$ by

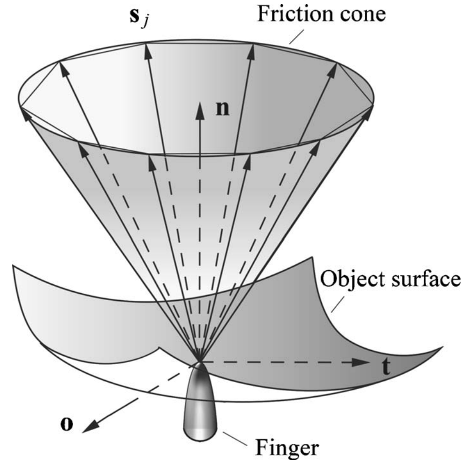

Fig. 1 Linearization of the friction cone at a contact point

$$\mathbf{s}_j = [1\ \mu\cos(2j\pi/n)\ \mu\sin(2j\pi/n)]^T \tag{2}$$

Thus $\mathbf{f}_i$ in the friction cone can be approximately represented by

$$\mathbf{f}_i = \sum_{j=1}^{n} \alpha_{ij}\mathbf{s}_j, \quad \alpha_{ij} \geqslant 0 \tag{3}$$

From Eqs. (1)–(3), f_{in}, f_{io}, and f_{it} are specified by

$$f_{in} = \sum_{j=1}^{n} \alpha_{ij}, \quad f_{io} = \mu\sum_{j=1}^{n} \alpha_{ij}\cos(2j\pi/n), \quad f_{it} = \mu\sum_{j=1}^{n} \alpha_{ij}\sin(2j\pi/n) \tag{4}$$

The wrench (a couple of force and moment applied at the origin of the object coordinate frame) produced by $\mathbf{f}_i$ is given by

$$\mathbf{w}_i = \mathbf{G}_i\mathbf{f}_i \tag{5}$$

where

$$\mathbf{G}_i = \begin{bmatrix} \mathbf{n}_i & \mathbf{o}_i & \mathbf{t}_i \\ \mathbf{r}_i \times \mathbf{n}_i & \mathbf{r}_i \times \mathbf{o}_i & \mathbf{r}_i \times \mathbf{t}_i \end{bmatrix}$$

Substituting Eq. (3) into Eq. (5) yields

$$\mathbf{w}_i = \sum_{j=1}^{n} \alpha_{ij}\mathbf{w}_{ij}, \quad \alpha_{ij} \geqslant 0$$

where

$$\mathbf{w}_{ij} = \mathbf{G}_i\mathbf{s}_j, \quad i = 1,2,\ldots,m, \quad j = 1,2,\ldots,n \tag{6}$$

The vector $\mathbf{w}_{ij}$ is called a primitive wrench. Thereby the resultant wrench applied by the hand is

$$\mathbf{w} = \sum_{i=1}^{m} \mathbf{w}_i = \sum_{i=1}^{m}\sum_{j=1}^{n} \alpha_{ij}\mathbf{w}_{ij}, \quad \alpha_{ij} \geqslant 0$$

A grasp is said to be force-closure if there always exist nonnegative reals α_{ij}, $i=1,2,\ldots,m$ and $j=1,2,\ldots,n$ such that $-\mathbf{w}_{\text{ext}} = \sum_{i=1}^{m}\sum_{j=1}^{n}\alpha_{ij}\mathbf{w}_{ij}$ for any $\mathbf{w}_{\text{ext}} \in \mathbb{R}^6$, which is equivalent to that the primitive wrenches positively span the whole wrench space [1]. Let $\mathcal{W}$ be the convex hull of the primitive wrenches:

$$\mathcal{W} = \left\{ \sum_{i=1}^{m}\sum_{j=1}^{n} \alpha_{ij}\mathbf{w}_{ij} \middle| \sum_{i=1}^{m}\sum_{j=1}^{n} \alpha_{ij} = 1,\ \alpha_{ij} \geqslant 0 \right\} \tag{7}$$

Not only the force-closure property but also the grasp quality can be revealed from $\mathcal{W}$ [2,4,16,17]. Noticing that $\mathcal{W}$ may be 6D or of lower dimension, in general we would discuss its relative interior as well as dimension rather than its interior. As the mathematical basis, we first extend the theorems on interior in convex analysis [38] to relative interior. Later, all of them will be used to solve the foregoing force-closure problems.

3 Results of Convex Analysis

Let S be a nonempty convex set in $\mathbb{R}^d$. The *dimension* of S is the dimension of its affine hull aff S, namely the dimension of the corresponding parallel subspace. The *relative interior* of S is the interior of S relative to aff S. In fact, the definition "relative interior" is an extension of the definition "interior." When aff $S=\mathbb{R}^d$, ri $S=$int S. As the former covers the latter, and we can regard the latter as a special case of the former. The set cl $S\backslash$ri S is called the relative boundary of S, denoted by rb S.

THEOREM 1. $\mathbf{0}\in$ int S *if and only if* dim $S=d$ *and* $\mathbf{0}\in$ ri S.

THEOREM 2. *If S is the convex hull of a finite set of points* $\mathbf{x}_1,\mathbf{x}_2,\ldots,\mathbf{x}_e$ *in* $\mathbb{R}^d$, *i.e.*, $S=\mathrm{conv}\{\mathbf{x}_1,\mathbf{x}_2,\ldots,\mathbf{x}_e\}$, *then any strictly positive convex combination of* $\mathbf{x}_1,\mathbf{x}_2,\ldots,\mathbf{x}_e$ *is a relative interior point of S, i.e.*, $\Sigma_{k=1}^{e}\lambda_k\mathbf{x}_k\in$ ri S *for any* $\lambda_1,\lambda_2,\ldots,\lambda_e>0$ *with* $\Sigma_{k=1}^{e}\lambda_k=1$.

To prove this theorem, we need two lemmas.

LEMMA 1. *If S is the convex hull of affinely independent points* $\mathbf{x}_1,\mathbf{x}_2,\ldots,\mathbf{x}_e$ *in* $\mathbb{R}^d$, *i.e.*, $S=\mathrm{conv}\{\mathbf{x}_1,\mathbf{x}_2,\ldots,\mathbf{x}_e\}$, *then any strictly positive convex combination of* $\mathbf{x}_1,\mathbf{x}_2,\ldots,\mathbf{x}_e$ *is a relative interior point of S, i.e.*, $\Sigma_{k=1}^{e}\lambda_k\mathbf{x}_k\in$ ri S *for any* $\lambda_1,\lambda_2,\ldots,\lambda_e>0$ *with* $\Sigma_{k=1}^{e}\lambda_k=1$.

Proof. Since $\mathbf{x}_1,\mathbf{x}_2,\ldots,\mathbf{x}_e$ are affinely independent, they constitute an affine basis of aff S; hence each point $\mathbf{x}\in$ aff S can be expressed by $\mathbf{x}=\Sigma_{k=1}^{e}\lambda_k\mathbf{x}_k$ with $\Sigma_{k=1}^{e}\lambda_k=1$, and the coefficients $\lambda_1,\lambda_2,\ldots,\lambda_e$ are unique. Therefore, we define

$$\varphi:\mathrm{aff}\, S\rightarrow\mathbb{R}^e$$

by letting

$$\varphi\left(\sum_{k=1}^{e}\lambda_k\mathbf{x}_k\right)=[\lambda_1\ \lambda_2\ \cdots\ \lambda_e]^T\text{ with }\sum_{k=1}^{e}\lambda_k=1$$

This is an affine mapping; in particular, it is continuous. Let

$$H_k=\{[\lambda_1\ \lambda_2\ \cdots\ \lambda_e]^T\in\mathbb{R}^e|\lambda_k>0\},\quad k=1,2,\ldots,e.$$

Then $H_1,H_2,\ldots,H_e$ are open halfspaces in $\mathbb{R}^e$; hence, by continuity, $\varphi^{-1}(H_1),\varphi^{-1}(H_2),\ldots,\varphi^{-1}(H_e)$ are open in aff S. Their intersection

$$\bigcap_{k=1}^{e}\varphi^{-1}(H_k)=\left\{\sum_{k=1}^{e}\lambda_k\mathbf{x}_k\in\mathbb{R}^d|\lambda_1,\lambda_2,\ldots,\lambda_e>0,\sum_{k=1}^{e}\lambda_k=1\right\}$$

is therefore also open in aff S. This in particular shows that the set $\cap_{k=1}^{e}\varphi^{-1}(H_k)$ is nonempty. Since $\cap_{k=1}^{e}\varphi^{-1}(H_k)$ is a set of positive convex combinations of $\mathbf{x}_1,\mathbf{x}_2,\ldots,\mathbf{x}_e$, we have $\cap_{k=1}^{e}\varphi^{-1}(H_k)\subset S$. In other words, S contains a nonempty set which is open in aff S, whence $\cap_{k=1}^{e}\varphi^{-1}(H_k)\subset$ ri S.

LEMMA 2. *If* $x_0\in$ ri S *and* $\mathbf{x}_1\in S$, *then* $(1-\lambda)\mathbf{x}_0+\lambda\mathbf{x}_1\in$ ri S *for all* $\lambda\in[0,1)$ [38].

Proof of theorem 2. Let $h=$dim S(=dim(aff S)). Then there exists $h+1$ affinely independent points from $\{\mathbf{x}_1,\mathbf{x}_2,\ldots,\mathbf{x}_e\}$; without loss of generality, say $\mathbf{x}_1,\mathbf{x}_2,\ldots,\mathbf{x}_{h+1}$. Let

$$S_1=\mathrm{conv}\{\mathbf{x}_1,\mathbf{x}_2,\ldots,\mathbf{x}_{h+1}\}\text{ and }S_2=\mathrm{conv}\{\mathbf{x}_{h+2},\mathbf{x}_{h+3},\ldots,\mathbf{x}_e\}$$

Then $S_1,S_2\subset S$ and dim(aff S_1)=dim $S_1=h$. Let

$$\mathbf{x}=\sum_{k=1}^{e}\lambda_k\mathbf{x}_k\text{ with }\lambda_1,\lambda_2,\ldots,\lambda_e>0\text{ and }\sum_{k=1}^{e}\lambda_k=1$$

This equation can be rewritten as

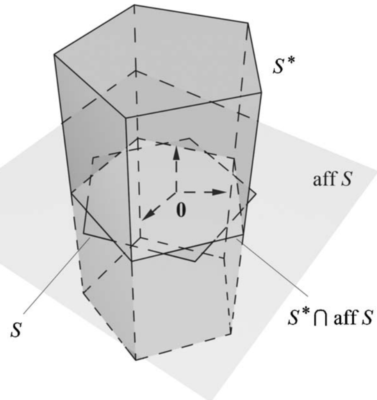

Fig. 2 The polar set of a compact convex set containing the origin as a relative interior point

$$\mathbf{x}=l_1\sum_{k=1}^{h+1}\frac{\lambda_k}{l_1}\mathbf{x}_k+l_2\sum_{k=h+2}^{e}\frac{\lambda_k}{l_2}\mathbf{x}_k=l_1\mathbf{y}+l_2\mathbf{z}$$

where $l_1=\Sigma_{k=1}^{h+1}\lambda_k$, $l_2=\Sigma_{k=h+2}^{e}\lambda_k$, $\mathbf{y}=\Sigma_{k=1}^{h+1}\lambda_k\mathbf{x}_k/l_1$, and $\mathbf{z}=\Sigma_{k=h+2}^{e}\lambda_k\mathbf{x}_k/l_2$. Note that $\mathbf{y}$ is a strictly positive convex combination of $\mathbf{x}_1,\mathbf{x}_2,\ldots,\mathbf{x}_{h+1}$, and from Lemma 1, $\mathbf{y}\in$ ri S_1. From aff $S_1\subset$ aff S and dim(aff S_1)=dim(aff S), we have aff S_1=aff S. But since $S_1\subset S$, it follows that $\mathbf{y}\in$ ri S. In addition, $\mathbf{z}$ is a convex combination of $\mathbf{x}_{h+2},\mathbf{x}_{h+3},\ldots,\mathbf{x}_e$; thus $\mathbf{z}\in S_2$, which implies $\mathbf{z}\in S$. Because $l_1>0$ and $l_1+l_2=1$, Lemma 2 ensures that $\mathbf{x}\in$ ri S.

The *polar set* S^* [38] of S is defined by

$$S^*=\{\mathbf{y}\in\mathbb{R}^d|\mathbf{x}^T\mathbf{y}\leqslant 1\text{ for all }\mathbf{x}\in S\}\tag{8}$$

THEOREM 3. *If* $\mathbf{0}\in S$, *then* $S^*=(S^*\cap\mathrm{aff}\,S)+(\mathrm{aff}\,S)^{\perp}$. *Furthermore, if S is compact and* $\mathbf{0}\in$ ri S, *then* $S^*\cap$ aff S *is a compact convex set in* aff S *and* $\mathbf{0}\in$ int S^*.

Proof. If $\mathbf{0}\in S$, aff S is a subspace of $\mathbb{R}^d$. Let $\mathbf{y}_1\in S^*\cap$ aff S and $\mathbf{y}_2\in(\mathrm{aff}\,S)^{\perp}$. $\mathbf{x}^T\mathbf{y}_1\leqslant 1$ and $\mathbf{x}^T\mathbf{y}_2=0$ for all $\mathbf{x}\in S$; thus $\mathbf{x}^T(\mathbf{y}_1+\mathbf{y}_2)\leqslant 1$, and $(S^*\cap\mathrm{aff}\,S)+(\mathrm{aff}\,S)^{\perp}\subset S^*$. Conversely, $\mathbf{y}\in S^*$ can be decomposed into $\mathbf{y}_1\in$ aff S and $\mathbf{y}_2\in(\mathrm{aff}\,S)^{\perp}$. For all $\mathbf{x}\in S$, $\mathbf{x}^T\mathbf{y}=\mathbf{x}^T\mathbf{y}_1\leqslant 1$; thus $\mathbf{y}_1\in S^*$. Hence $\mathbf{y}_1\in S^*\cap$ aff S, and $S^*\subset(S^*\cap\mathrm{aff}\,S)+(\mathrm{aff}\,S)^{\perp}$. Therefore, $S^*=(S^*\cap\mathrm{aff}\,S)+(\mathrm{aff}\,S)^{\perp}$, as shown in Fig. 2.

In addition, if S is a compact convex set in $\mathbb{R}^d$ with $\mathbf{0}\in$ int S, S^* is a compact convex set in $\mathbb{R}^d$ with $\mathbf{0}\in$ int S^* [38]. In general, if S is compact and $\mathbf{0}\in$ ri S, $S^*\cap$ aff S is a compact convex set in aff S and $\mathbf{0}$ is an interior point of S^* relative to aff S. From $S^*=(S^*\cap\mathrm{aff}\,S)+(\mathrm{aff}\,S)^{\perp}$, dim $S^*=d$. Thus $\mathbf{0}\in$ int S^*.

The *support function* p_S [38] of S is the real-valued function defined by

$$p_S(\mathbf{z})=\sup_{\mathbf{x}\in S}\mathbf{z}^T\mathbf{x}\tag{9}$$

for all $\mathbf{z}\in\mathbb{R}^d$ for which the supremum is finite. Let p_{S^*} be the support function of S^*. In the following, we assume that S is a nonempty compact convex set with $\mathbf{0}\in$ ri S.

THEOREM 4. $p_{S^*}(\mathbf{z})$ *is finite if and only if* $\mathbf{z}\in$ aff S. *Moreover, if* $\mathbf{z}\in$ aff S, *then* $p_{S^*}(\mathbf{z})=p_{S^*\cap\mathrm{aff}\,S}(\mathbf{z})$ *and there is* $\mathbf{y}_z\in S^*\cap$ aff S *such that* $p_{S^*}(\mathbf{z})=\mathbf{z}^T\mathbf{y}_z$. *If* $\mathbf{z}$ *is nonzero, then* $p_{S^*}(\mathbf{z})>0$.

Proof. From Theorem 3 it follows that any $\mathbf{y}\in S^*$ can be decomposed into $\mathbf{y}_1\in S^*\cap$ aff S and $\mathbf{y}_2\in(\mathrm{aff}\,S)^{\perp}$; thus $\mathbf{z}^T\mathbf{y}=\mathbf{z}^T\mathbf{y}_1+\mathbf{z}^T\mathbf{y}_2$ for any $\mathbf{y}\in S^*$. If $\mathbf{z}\in$ aff S, then $\mathbf{z}^T\mathbf{y}=\mathbf{z}^T\mathbf{y}_1$, which implies that $p_{S^*}(\mathbf{z})=p_{S^*\cap\mathrm{aff}\,S}(\mathbf{z})$. Due to the compactness of $S^*\cap$ aff S (see Theorem 3) and the continuity of the inner product, $p_{S^*}(\mathbf{z})$ is finite and there exists a point $\mathbf{y}_z\in S^*\cap$ aff S such that $p_{S^*}(\mathbf{z})=\mathbf{z}^T\mathbf{y}_z$. Conversely, if $\mathbf{z}\notin$ aff S, then $\mathbf{z}$ can be decomposed into $\mathbf{z}_1\in$ aff S and $\mathbf{z}_2\in(\mathrm{aff}\,S)^{\perp}$, where $\mathbf{z}_2$ is nonzero, so $\mathbf{z}^T\mathbf{y}=\mathbf{z}_1^T\mathbf{y}_1+\mathbf{z}_2^T\mathbf{y}_2$. Since $\mathbf{z}_1^T\mathbf{y}_1$

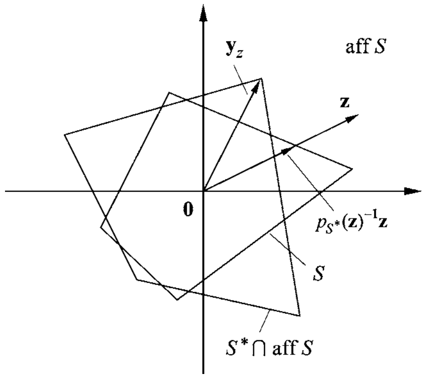

Fig. 3 Illustration of Theorem 5. The point $p_{S^*}(\mathbf{z})^{-1}\mathbf{z}$ is on the relative boundary of S.

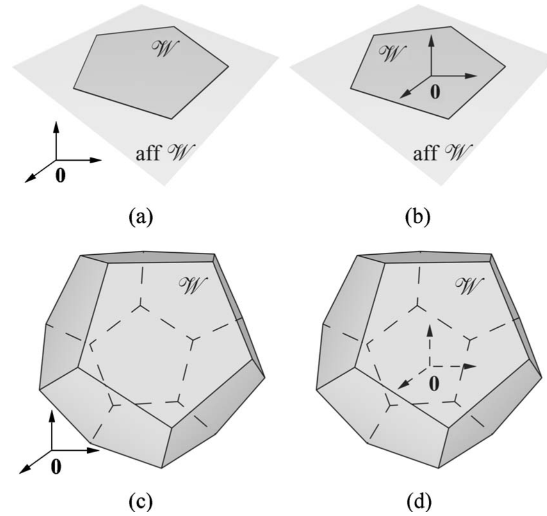

Fig. 4 Classification of $\mathcal{W}$. (*a*) dim $\mathcal{W}<6$ and $\mathbf{0}\notin$ aff $\mathcal{W}$. (*b*) dim $\mathcal{W}<6$ and $\mathbf{0}\in$ aff $\mathcal{W}$. (*c*) dim $\mathcal{W}=6$ and $\mathbf{0}\notin$ ri $\mathcal{W}$. (*d*) dim $\mathcal{W}=6$ and $\mathbf{0}\in$ ri$\mathcal{W}$.

is finite for all $\mathbf{y}_1\in S^*\cap\operatorname{aff} S$ while the supremum of $\mathbf{z}_2^T\mathbf{y}_2$ on $\mathbf{y}_2\in(\operatorname{aff} S)^\perp$ takes on arbitrarily large values, the supremum of $\mathbf{z}^T\mathbf{y}$ on $\mathbf{y}\in S^*$ is infinite. This proof can be illustrated in Fig. 2. Furthermore, from Theorem 3, $\mathbf{0}\in\operatorname{int} S^*$. Then for any nonzero $\mathbf{z}\in\operatorname{aff} S$, we may always find $\mathbf{y}\in S^*$ such that $\mathbf{z}^T\mathbf{y}>0$; thus $p_{S^*}(\mathbf{z})>0$.

THEOREM 5. *Let* $\mathbf{z}$ *be a point in* aff S *other than* $\mathbf{0}$. *Then* $p_{S^*}(\mathbf{z})^{-1}\mathbf{z}\in\operatorname{rb} S$.

Proof. From the definition of p_{S^*}, $\mathbf{z}^T\mathbf{y}\leqslant p_{S^*}(\mathbf{z})$ for all $\mathbf{y}\in S^*$. From Theorem 4, $p_{S^*}(\mathbf{z})>0$. Then $\mathbf{y}^T p_{S^*}(\mathbf{z})^{-1}\mathbf{z}\leqslant 1$ for all $\mathbf{y}\in S^*$, which means $p_{S^*}(\mathbf{z})^{-1}\mathbf{z}\in(S^*)^*$. Since S is closed and contains $\mathbf{0}$, we have $(S^*)^*=S$ [38], and $p_{S^*}(\mathbf{z})^{-1}\mathbf{z}\in S$. Let $B(p_{S^*}(\mathbf{z})^{-1}\mathbf{z},r)$ be a closed ball in aff S of radius $r>0$ centered at $p_{S^*}(\mathbf{z})^{-1}\mathbf{z}$. Let $\mathbf{x}=p_{S^*}(\mathbf{z})^{-1}\mathbf{z}+r\mathbf{z}/\|\mathbf{z}\|$. Obviously, $\mathbf{x}\in B(p_{S^*}(\mathbf{z})^{-1}\mathbf{z},r)$. Because $\mathbf{y}_z^T\mathbf{x}=1+rp_{S^*}(\mathbf{z})/\|\mathbf{z}\|>1$ where $\mathbf{y}_z\in S^*\cap\operatorname{aff} S$ such that $p_{S^*}(\mathbf{z})=\mathbf{z}^T\mathbf{y}_z$ (see Theorem 4), we have $\mathbf{x}\notin(S^*)^*$, i.e., $\mathbf{x}\notin S$. Hence $p_{S^*}(\mathbf{z})^{-1}\mathbf{z}\notin\operatorname{ri} S$, and $p_{S^*}(\mathbf{z})^{-1}\mathbf{z}\in\operatorname{rb} S$. This proof is illustrated in Fig. 3.

THEOREM 6. *Let* $\mathbf{z}$ *be a point in* aff S. *Then* $\mathbf{z}\in\operatorname{ri} S$ *if and only if* $p_{S^*}(\mathbf{z})<1$.

Proof. Suppose that $\mathbf{z}$ is a point other than $\mathbf{0}$. Theorem 5 asserts that $p_{S^*}(\mathbf{z})^{-1}\mathbf{z}\in\operatorname{rb} S$. If $p_{S^*}(\mathbf{z})<1$, $\mathbf{z}$ is strictly between $\mathbf{0}$ and $p_{S^*}(\mathbf{z})^{-1}\mathbf{z}$, and from Lemma 2 we obtain $\mathbf{z}\in\operatorname{ri} S$. Theorem 4 affirms that $p_{S^*}(\mathbf{z})>0$. If $p_{S^*}(\mathbf{z})\geqslant 1$, then $\mathbf{z}$ lies on the relative boundary of S or outside S. When $\mathbf{z}$ is just $\mathbf{0}$, $p_{S^*}(\mathbf{z})=0<1$. Conversely, $p_{S^*}(\mathbf{z})=0$ implies $\mathbf{z}=\mathbf{0}\in\operatorname{ri} S$.

4 Force-Closure Conditions and Test

4.1 Classification of $\mathcal{W}$. The convex hull of the primitive wrenches, denoted by $\mathcal{W}$, has been used in force-closure analysis for a long time. However, its dimension was always neglected or assumed to be 6 in the 3D work space. In fact, the dimension of $\mathcal{W}$ may be less than 6.

By the dimension and the relative position to the origin $\mathbf{0}$, we classify $\mathcal{W}$ into four categories:

(a) dim $\mathcal{W}<6$ and $\mathbf{0}\notin$ aff $\mathcal{W}$ (Fig. 4(*a*)).
(b) dim $\mathcal{W}<6$ and $\mathbf{0}\in$ aff $\mathcal{W}$ (Fig. 4(*b*)).
(c) dim $\mathcal{W}=6$ and $\mathbf{0}\notin$ ri $\mathcal{W}$ (Fig. 4(*c*)).
(d) dim $\mathcal{W}=6$ and $\mathbf{0}\in$ ri $\mathcal{W}$ (Fig. 4(*d*)).

When ignoring the dimension of $\mathcal{W}$, the ray-shooting based algorithm [4] does not have a solution in case (*a*), and mistakes $\mathbf{0}$ for an interior point of $\mathcal{W}$ in case (*b*) if $\mathbf{0}\in$ ri $\mathcal{W}$. Hence, in what follows, we take into account the dimension of $\mathcal{W}$ and suggest a way to avoid these errors.

4.2 Force-Closure Conditions. Our conditions originate from Mishra et al. [2], who wrote:

PROPOSITION 1. *A grasp is force-closure if and only if* $\mathbf{0}\in\operatorname{int}\mathcal{W}$.

Theorem 1 gives directly:

PROPOSITION 2. $\mathbf{0}\in\operatorname{int}\mathcal{W}$ *if and only if* dim $\mathcal{W}=6$ *and* $\mathbf{0}\in$ ri $\mathcal{W}$ *(Fig. 4(d))*.

The convex cone determined by $\mathcal{W}$ and $\mathbf{0}$ consists of the resultant wrenches that can be generated by the grasp. If dim $\mathcal{W}<6$ and $\mathbf{0}\in$ ri $\mathcal{W}$, then the grasp can generate resultant wrenches in a proper subspace of $\mathbb{R}^6$, namely aff $\mathcal{W}$, as depicted in Fig. 4(*b*). Such a grasp is said to be *partially force-closure* [10]. Let $\mathbf{w}_c$ be the centroid of the primitive wrenches $\mathbf{w}_{ij}$ and $\mathcal{T}$ the translate of $\mathcal{W}$ by $-\mathbf{w}_c$

$$\mathbf{w}_c=\frac{1}{mn}\sum_{i=1}^{m}\sum_{j=1}^{n}\mathbf{w}_{ij} \tag{10}$$

$$\mathcal{T}=\mathcal{W}-\mathbf{w}_c \tag{11}$$

From Eq. (7) and Theorem 2 it follows that $\mathbf{w}_c\in$ ri $\mathcal{W}$. Thus $\mathcal{T}$ is a compact convex set in $\mathbb{R}^6$ with $\mathbf{0}\in$ ri $\mathcal{T}$, and aff $\mathcal{T}$ is a subspace of $\mathbb{R}^6$. Furthermore, we readily have

PROPOSITION 3. *The following statements are true: (1)* dim $\mathcal{W}=6$ *if and only if* dim $\mathcal{T}=6$; *(2)* $\mathbf{0}\in$ ri $\mathcal{W}$ *if and only if* $-\mathbf{w}_c\in$ ri $\mathcal{T}$.

According to Proposition 3, the properties of $\mathcal{W}$ can be investigated from $\mathcal{T}$. Let

$$\mathbf{T}=[\mathbf{w}_{11}-\mathbf{w}_c\ \cdots\ \mathbf{w}_{ij}-\mathbf{w}_c\ \cdots\ \mathbf{w}_{mn}-\mathbf{w}_c]\in\mathbb{R}^{6\times mn} \tag{12}$$

PROPOSITION 4. dim $\mathcal{T}=6$ *if and only if rank* $\mathbf{T}=6$.

Proof. As aff $\mathcal{T}$ is a subspace of $\mathbb{R}^6$ and is equal to the range of the matrix $\mathbf{T}$, the dimension of aff $\mathcal{T}$ equals the rank of $\mathbf{T}$, i.e., dim $\mathcal{T}=$ rank $\mathbf{T}$.

Let $\mathcal{T}^*$ be the polar set of $\mathcal{T}$. From Eqs. (7), (8), and (11), $\mathcal{T}^*$ can be expressed by

$$\mathcal{T}^*=\{\mathbf{u}\in\mathbb{R}^6|(\mathbf{w}_{ij}-\mathbf{w}_c)^T\mathbf{u}\leqslant 1,\ i=1,2,\ldots,m,\ j=1,2,\ldots,n\} \tag{13}$$

Let p denote the support function of $\mathcal{T}^*$:

$$p(\mathbf{w})=\sup_{\mathbf{u}\in\mathcal{T}^*}\mathbf{w}^T\mathbf{u} \tag{14}$$

for all $\mathbf{w}\in\mathbb{R}^6$ for which the supremum is finite.

PROPOSITION 5. $-\mathbf{w}_c\in$ ri $\mathcal{T}$ *if and only if* $p(-\mathbf{w}_c)<1$.

Proof. If $p(-\mathbf{w}_c)<1$, then from Theorem 4 we have $-\mathbf{w}_c$

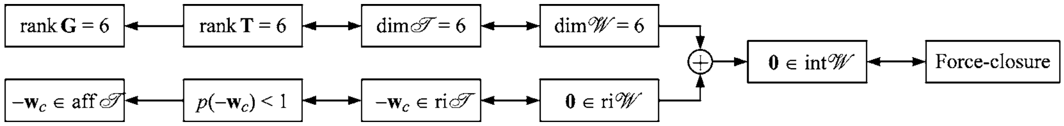

Fig. 5 Logic relations among various force-closure conditions in Sec. 4.2

$\in \operatorname{aff} \mathcal{T}$. From Theorem 6 it is straightforward that $-\mathbf{w}_c \in \operatorname{ri} \mathcal{T}$ if and only if $p(-\mathbf{w}_c) < 1$.

The above force-closure conditions and their relations are summarized in Fig. 5. In addition, it especially needs to be cautious about:

1. $\dim \mathcal{W}=6$ implies rank $\mathbf{G}=6$, but the converse does not hold true. The dimension of $\mathcal{W}$ is equal to the rank of $\mathbf{T}$ and may be *less* than the rank of $\mathbf{G}$.
2. $p(-\mathbf{w}_c) < 1$ implies $-\mathbf{w}_c \in \operatorname{aff} \mathcal{T}$, but $-\mathbf{w}_c \in \operatorname{aff} \mathcal{T}$ must be confirmed prior to computing $p(-\mathbf{w}_c)$. $p(-\mathbf{w}_c)$ is finite and can be computed only if $-\mathbf{w}_c \in \operatorname{aff} \mathcal{T}$.

4.3 Force-Closure Test Algorithm. Referring to Fig. 5, the force-closure test can be formulated as:

Step 1: Calculate the primitive wrenches $\mathbf{w}_{ij}$ by Eqs. (2) and (6).

Step 2: Compute the centroid $\mathbf{w}_c$ by Eq. (10).

Step 3: Construct the matrix $\mathbf{T}$ by Eq. (12) and calculate its rank.

Step 4: Determine if $-\mathbf{w}_c \in \operatorname{aff} \mathcal{T}$. Since $\operatorname{aff} \mathcal{T}$ equals the range of $\mathbf{T}$, $-\mathbf{w}_c \in \operatorname{aff} \mathcal{T}$ if and only if the linear system $\mathbf{T}\mathbf{z}=-\mathbf{w}_c$ is consistent, or $\|\mathbf{T}\mathbf{T}^{+}\mathbf{w}_c-\mathbf{w}_c\|=0$, where $\mathbf{T}^{+}$ is the pseudoinverse of $\mathbf{T}$. If $\|\mathbf{T}\mathbf{T}^{+}\mathbf{w}_c-\mathbf{w}_c\|=0$, then go to Step 5; otherwise the algorithm terminates.

Step 5: Compute $p(-\mathbf{w}_c)$. From Eqs. (13) and (14), it is formulated as an LP problem:

$$\begin{cases} \text{Maximize } -\mathbf{w}_c^T\mathbf{u} \\ \text{subject to } (\mathbf{w}_{ij}-\mathbf{w}_c)^T\mathbf{u} \leqslant 1, \; i=1,2,\ldots,m, \; j=1,2,\ldots,n \end{cases} \tag{15}$$

The algorithm ends.

The algorithm turns out four types of results corresponding to the foregoing categories of $\mathcal{W}$:

(a) rank $\mathbf{T}<6$ and $\|\mathbf{T}\mathbf{T}^{+}\mathbf{w}_c-\mathbf{w}_c\| \neq 0$.
(b) rank $\mathbf{T}<6$ and $\|\mathbf{T}\mathbf{T}^{+}\mathbf{w}_c-\mathbf{w}_c\|=0$.
(c) rank $\mathbf{T}=6$ and $p(-\mathbf{w}_c) \geqslant 1$.
(d) rank $\mathbf{T}=6$ and $p(-\mathbf{w}_c) < 1$ (force-closure).

This formulation of force-closure test is closely related to the typical ray-shooting problem [4], i.e., a problem of finding the intersection of a ray with the boundary of a polytope. Denote the ray from the point $\mathbf{w}_c$ to the origin $\mathbf{0}$ by

$$\mathcal{R} = \{-\beta\mathbf{w}_c + \mathbf{w}_c | \beta \geqslant 0\}$$

where $\mathbf{w}_c \neq \mathbf{0}$. The condition $-\mathbf{w}_c \in \operatorname{aff} \mathcal{T}$, determined by $\|\mathbf{T}\mathbf{T}^{+}\mathbf{w}_c-\mathbf{w}_c\|=0$, ensures that $\mathcal{R}$ is contained in $\operatorname{aff} \mathcal{T}$ and intersects with $\operatorname{rb} \mathcal{W}$, which in turn guarantees that $p(-\mathbf{w}_c)$ is finite. Hence, since $\mathcal{T}^*$ is nonempty, the LP problem (15) always has solution and can be solved in $O(mn)$ time. In fact, intersection happens at the point $-p(-\mathbf{w}_c)^{-1}\mathbf{w}_c+\mathbf{w}_c$, as shown in Fig. 6. Then $p(-\mathbf{w}_c)$ equals the ratio of the distance between $\mathbf{w}_c$ and $\mathbf{0}$ to the one between $\mathbf{w}_c$ and the intersection point. Therefore, $p(-\mathbf{w}_c)<1$ means $\mathbf{0} \in \operatorname{ri} \mathcal{W}$. This geometric insight into $p(-\mathbf{w}_c)$ first helps us skip the computation of the distances and simplify the original ray-shooting approach to force-closure test [4,34]. Moreover, $p(-\mathbf{w}_c)$ intuitively suggests a risk of losing force-closure, or its reciprocal gives a safety factor of force-closure.

5 Optimal Grasp Planning

5.1 Performance Index of a Grasp Configuration. The previous section indicates that $p(-\mathbf{w}_c)$ can be applied to reflecting the force-closure property of grasps. Hereafter, we give a further physical interpretation of $p(-\mathbf{w}_c)$. Assume that $\dim \mathcal{W}=6$, and then the force-closure property is entirely represented by $p(-\mathbf{w}_c)$.

Equation (10) shows that $\mathbf{w}_c$ is the convex combination of $\mathbf{w}_{ij}$ with the coefficients

$$\alpha_{c,ij} = \frac{1}{mn}, \quad i=1,2,\ldots,m, \quad j=1,2,\ldots,n \tag{16}$$

Substituting Eq. (16) into Eq. (4) with $\Sigma_{j=1}^{n}\cos(2j\pi/n) = \Sigma_{j=1}^{n}\sin(2j\pi/n)=0$ yields

$$f_{c,in} = \frac{1}{m}, \quad f_{c,io}=f_{c,it}=0 \tag{17}$$

Hence, $\mathbf{w}_c$ is the resultant wrench of the contact forces $\mathbf{f}_{c,i} = [1/m \; 0 \; 0]^T$, $i=1,2,\ldots,m$, i.e.,

$$\mathbf{w}_c = \sum_{i=1}^{m} \mathbf{G}_i\mathbf{f}_{c,i} \tag{18}$$

When $p(-\mathbf{w}_c) \geqslant 1$, $\mathbf{0} \notin \operatorname{ri} \mathcal{W}$ and the grasp is not force-closure.

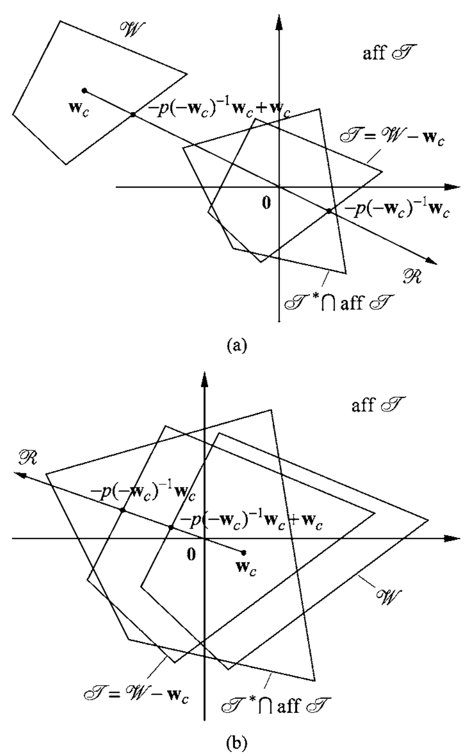

Fig. 6 Point $-p(-\mathbf{w}_c)^{-1}\mathbf{w}_c+\mathbf{w}_c$ is the intersection of the ray $\dot{\mathcal{R}}$ with the relative boundary of $\mathcal{W}$. (*a*) If $p(-\mathbf{w}_c) \geqslant 1$, then $\mathbf{0} \notin \operatorname{ri} \mathcal{W}$. (*b*) If $0<p(-\mathbf{w}_c)<1$, then $\mathbf{0} \in \operatorname{ri} \mathcal{W}$.

$p(-\mathbf{w}_c)$ implies how far the grasp is away from force-closure.

Let us pay more attention to the case of $p(-\mathbf{w}_c)<1$. Then $\mathbf{0} \in \mathrm{ri}\,\mathcal{W}$, and the affine hull $\mathrm{aff}\,\mathcal{W}$ is a subspace of $\mathbb{R}^6$, which comprises the resultant wrenches that the grasp can apply on the gripped object. From $\mathbf{w}_c \in \mathrm{aff}\,\mathcal{W}$ it follows that $-\mathbf{w}_c \in \mathrm{aff}\,\mathcal{W}$, i.e., there exist non-negative reals λ_{ij}, $i=1,2,\ldots,m$ and $j=1,2,\ldots,n$ such that

$$-\mathbf{w}_c = \sum_{i=1}^{m}\sum_{j=1}^{n}\lambda_{ij}\mathbf{w}_{ij} \tag{19}$$

This equation can be rewritten as

$$-\mathbf{w}_c = \sigma\sum_{i=1}^{m}\sum_{j=1}^{n}\frac{\lambda_{ij}}{\sigma}\mathbf{w}_{ij} = \sigma\mathbf{w}_a \tag{20}$$

where

$$\sigma = \sum_{i=1}^{m}\sum_{j=1}^{n}\lambda_{ij} \tag{21}$$

$$\mathbf{w}_a = \sum_{i=1}^{m}\sum_{j=1}^{n}\frac{\lambda_{ij}}{\sigma}\mathbf{w}_{ij} \tag{22}$$

From Eq. (4), σ specifies the sum of the normal force components for all contacts. Equation (20) indicates that $\mathbf{w}_a \in \mathcal{R}$ and

$$\sigma = \frac{\|\mathbf{w}_c\|}{\|\mathbf{w}_a\|} \tag{23}$$

From Eqs. (7), (21), and (22) we see that $\mathbf{w}_a \in \mathcal{W}$. Thus from Eq. (23), σ attains its minimum value $\underline{\sigma}$ when $\mathbf{w}_a$ is the intersection point of $\mathcal{R}$ with $\mathrm{rb}\,\mathcal{W}$ (Fig. 6(*b*)), i.e.,

$$\mathbf{w}_a = -p(-\mathbf{w}_c)^{-1}\mathbf{w}_c + \mathbf{w}_c$$

$$\underline{\sigma} = \frac{\|\mathbf{w}_c\|}{\|-p(-\mathbf{w}_c)^{-1}\mathbf{w}_c + \mathbf{w}_c\|} = \frac{1}{p(-\mathbf{w}_c)^{-1}-1}$$

The derivative of $\underline{\sigma}$ with respect to $p(-\mathbf{w}_c)$ is

$$\frac{d\underline{\sigma}}{dp(-\mathbf{w}_c)} = \frac{1}{[1-p(-\mathbf{w}_c)]^2} > 0 \tag{24}$$

This means that $\underline{\sigma}$ is increasing on $p(-\mathbf{w}_c)\in[0,1)$.

Suppose that $\underline{\alpha}_{c,ij}$, $i=1,2,\ldots,m$ and $j=1,2,\ldots,n$ are non-negative coefficients satisfying Eq. (19) with $\underline{\sigma}=\sum_{i=1}^{m}\sum_{j=1}^{n}\underline{\alpha}_{c,ij}$. Substituting $\underline{\alpha}_{c,ij}$, $j=1,2,\ldots,n$ into Eq. (3) yields the contact forces $\underline{\mathbf{f}}_{c,i}$ satisfying

$$-\mathbf{w}_c = \sum_{i=1}^{m}\mathbf{G}_i\underline{\mathbf{f}}_{c,i}, \tag{25}$$

$$\underline{f}_{c,in} \geqslant 0, \tag{26}$$

$$(\underline{f}_{c,io})^2 + (\underline{f}_{c,it})^2 \leqslant (\mu\underline{f}_{c,in})^2 \tag{27}$$

$$\sum_{i=1}^{m}\underline{f}_{c,in} = \underline{\sigma} \tag{28}$$

Let $\mathbf{f}_{\mathrm{int}}=[\mathbf{f}_{\mathrm{int},1}^T\ \mathbf{f}_{\mathrm{int},2}^T\ \cdots\ \mathbf{f}_{\mathrm{int},m}^T]^T$ where

$$\mathbf{f}_{\mathrm{int},i} = \mathbf{f}_{c,i} + \underline{\mathbf{f}}_{c,i} \tag{29}$$

Substituting Eq. (17) into Eq. (29) leads to

$$f_{\mathrm{int},in} = \underline{f}_{c,in} + \frac{1}{m}, \quad f_{\mathrm{int},io} = \underline{f}_{c,io}, \quad f_{\mathrm{int},it} = \underline{f}_{c,it} \tag{30}$$

Combining Eqs. (18), (25), and (29) indicates

$$\sum_{i=1}^{m}\mathbf{G}_i\mathbf{f}_{\mathrm{int},i} = \mathbf{0} \tag{31}$$

From Eqs. (26), (27), and (30), we obtain

$$f_{\mathrm{int},in} > \underline{f}_{c,in} \geqslant 0 \tag{32}$$

$$f_{\mathrm{int},io}^2 + f_{\mathrm{int},it}^2 = (\underline{f}_{c,io})^2 + (\underline{f}_{c,it})^2 \leqslant (\mu\underline{f}_{c,in})^2 < \mu^2 f_{\mathrm{int},in}^2 \tag{33}$$

Equation (31) means that $\mathbf{f}_{\mathrm{int}}$ is an *internal force*, while Eqs. (32) and (33) indicate that $\mathbf{f}_{\mathrm{int},i}$ is strictly inside the friction cone. Hence $\mathbf{f}_{\mathrm{int}}$ is a *strictly internal force* [6–10].

Let

$$\xi_i = \frac{\sqrt{f_{\mathrm{int},io}^2 + f_{\mathrm{int},it}^2}}{\mu f_{\mathrm{int},in}} \quad \text{for } i=1,2,\ldots,m \tag{34}$$

The value ξ_i implies the inclination angle of $\mathbf{f}_{\mathrm{int},i}$. Smaller values ξ_i, $i=1,2,\ldots,m$ mean higher grasp stability [8]. In grasp planning, we hope ξ_i as small as possible.

Substituting Eqs. (30) and (33) into Eq. (34) yields

$$\xi_i \leqslant \bar{\xi}_i \tag{35}$$

where

$$\bar{\xi}_i = \frac{\underline{f}_{c,in}}{\underline{f}_{c,in} + 1/m} \tag{36}$$

From Eqs. (35) and (36), $\bar{\xi}_i$ is an upper bound of ξ_i and increasing on $\underline{f}_{c,in}$. Minimizing $\underline{f}_{c,in}$ will minimize $\bar{\xi}_i$, which in turn reduces ξ_i. However, note that minimization of $\underline{f}_{c,in}$, $i=1,2,\ldots,m$ is a *multiobjective optimization problem (MOP)*. The most common method in MOP is the *point estimate weighted-sums approach* [39], which characterizes the noninferior solution in terms of the optimal solution of a composite objective function. Each objective is multiplied by a strictly positive scalar weight and the weighted objectives sum into the composite objective function. It is natural to take the weights of $\underline{f}_{c,in}$, $i=1,2,\ldots,m$ equally, so all of them are taken to be unity. Then the composite objective function is just $\underline{\sigma}$, as given by Eq. (28). Hence we may reduce ξ_i by minimizing $\underline{\sigma}$. From Eq. (24), this can be done by minimizing $p(-\mathbf{w}_c)$.

Therefore, $p(-\mathbf{w}_c)$ is relevant to the inclination angles of contact forces, and a small $p(-\mathbf{w}_c)$ benefits the grasp stability.

5.2 Constraints on the Grasp Configuration. First, the contact points should be restricted within some smooth pieces of the object surface. If a contact is located at a singular point, then $\mathbf{n}_i, \mathbf{o}_i, \mathbf{t}_i$ therein are uncertain and the grasp matrix $\mathbf{G}_i$ cannot be formulated. We denote this constraint by $\mathbf{r}_i \in R_i$, $i=1,2,\ldots,m$ where points in region R_i are nonsingular.

Second, $\dim\mathcal{W}=6$ is necessary to force-closure (Fig. 5). Herein we propose two necessary conditions for $\dim\mathcal{W}=6$, which are directly related to the grasp configuration. If these conditions are fulfilled, then $\dim\mathcal{W}=6$ in general.

PROPOSITION 6. $\dim\mathcal{W}=6$ *only if the following conditions are both satisfied: (1) at least three contact points are noncollinear; (2) at least two unit inward normals are different*.

Proof. If condition (1) is not satisfied, i.e., all the contact points are collinear, then $\mathrm{rank}\,\mathbf{G}=5$ [40]. As $\mathcal{W}$ lies in the range of $\mathbf{G}$, $\dim\mathcal{W}\leqslant\mathrm{rank}\,\mathbf{G}<6$.

Suppose that condition (2) is not satisfied, i.e., $\mathbf{n}_i=\mathbf{n}_1$ for all $i=2,3,\ldots,m$. Then $\mathbf{o}_i=\mathbf{o}_1$ and $\mathbf{t}_i=\mathbf{t}_1$ for $i=2,3,\ldots,m$. Applying elementary column operations to the matrix $\mathbf{T}$, we obtain

$$\begin{aligned}\tilde{\mathbf{T}} &= [\mathbf{0}\ \mathbf{w}_{12}-\mathbf{w}_{11}\cdots\mathbf{w}_{1\mathbf{n}}-\mathbf{w}_{11}\ \mathbf{w}_{21}-\mathbf{w}_{11}\cdots\mathbf{w}_{mn}-\mathbf{w}_{1n}]\\ &= [\mathbf{0}\ \mathbf{G}_1\ (\mathbf{s}_2-\mathbf{s}_1)\cdots\mathbf{G}_1\ (\mathbf{s}_n-\mathbf{s}_1)(\mathbf{G}_2-\mathbf{G}_1)\mathbf{s}_1\cdots(\mathbf{G}_m-\mathbf{G}_1)\mathbf{s}_n]\end{aligned}$$

Apparently, $\mathrm{rank}\,\mathbf{T}=\mathrm{rank}\,\tilde{\mathbf{T}}$. Partition $\tilde{\mathbf{T}}$ as

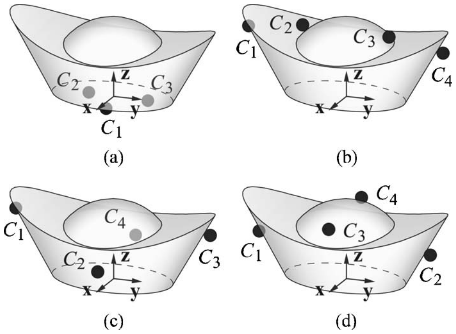

Fig. 7 Gold ingot used as money in feudal China

$$\tilde{\mathbf{T}} = \begin{bmatrix} \tilde{\mathbf{T}}_{11} & \tilde{\mathbf{T}}_{12} \\ \tilde{\mathbf{T}}_{21} & \tilde{\mathbf{T}}_{22} \end{bmatrix}$$

where $\tilde{\mathbf{T}}_{11}, \tilde{\mathbf{T}}_{21} \in \mathbb{R}^{3\times n}$ and $\tilde{\mathbf{T}}_{12}, \tilde{\mathbf{T}}_{22} \in \mathbb{R}^{3\times(m-1)n}$. Note that $\tilde{\mathbf{T}}_{12} = \mathbf{0}$ and rank $\tilde{\mathbf{T}}_{11} < 3$. Thus dim $\mathcal{W}$=rank $\mathbf{T} < 6$.

To comply with condition (1), one may choose R_i for three contacts such that their positions $\mathbf{r}_i \in R_i$ are noncollinear. Condition (2) can be treated in the same manner.

5.3 Grasp Planning Algorithm. Taking the above constraints into account, the optimal grasp planning problem is formulated as the following optimization problem, where $p(-\mathbf{w}_c)$ serves as the performance index:

$$\begin{cases} \text{Minimize } p(-\mathbf{w}_c) \\ \text{subject to } \mathbf{r}_i \in R_i, i = 1,2, \ldots, m \end{cases} \tag{37}$$

The iterative procedure of Eq. (37) can be divided into two phases. When $p(-\mathbf{w}_c) \geqslant 1$, the grasp is not force-closure. As $p(-\mathbf{w}_c)$ decreases to unity, $-p(-\mathbf{w}_c)^{-1}\mathbf{w}_c + \mathbf{w}_c$ is getting towards $\mathbf{0}$ and $\mathbf{0}$ is getting towards rb $\mathcal{W}$ (Fig. 6(*a*)). This means that the grasp is approaching force-closure. When $p(-\mathbf{w}_c) < 1$, the grasp is force-closure. As $p(-\mathbf{w}_c)$ keeps decreasing, the inclination angles of internal forces can be smaller and the grasp becomes more stable.

Different from the algorithm [32], this one considers the grasp stability in addition to the intuitive safety of force-closure. The performance index can be computed in $O(mn)$ time such that the algorithm is more efficient than the others [16,17]. Moreover, the planning algorithm can be applied to arbitrary 3D objects with piecewise smooth surface.

In addition, notice that the goal of fixture design is similar to grasp planning, i.e., positioning a number of contacts properly on the object surface to immobilize the object and equivalently to equilibrate any external wrenches on the object. The force-closure property, including form-closure as a frictionless case, is a basic requirement of both topics. Hence the ray-shooting approach is also available for fixture design. Such an application can be found in [33]. However, the optimization criterion of fixturing considers easy access or position accuracy rather than stability. Owing to this, the value of $p(-\mathbf{w}_c)$ may appear in the constraint other than the performance index.

6 Numerical Examples

We implement the proposed algorithms using MATLAB on a Pentium-M notebook and demonstrate their efficiency with two examples. The friction coefficient is assumed to be μ=0.3 and each friction cone is represented by a 100-sided polyhedral convex cone.

Example 1. As depicted in Fig. 7, a cast gold ingot may be fixtured differently for removing the surplus gold over the specified weight. The more surface the deburring instrument can access, the easier this work will be. Therefore we try to use less fixels. Yet force-closure must be ensured. First, the ingot is supported by three fixels (Fig. 7(*a*)):

$$\mathbf{r}_1 = [5\ 0\ 0]^T, \quad \mathbf{r}_2 = [-5\ \ -10\ 0]^T, \quad \mathbf{r}_3 = [-5\ 10\ 0\ ]^T$$

$$\mathbf{n}_1 = [0\ 0\ 1]^T, \quad \mathbf{n}_2 = [0\ 0\ 1]^T, \quad \mathbf{n}_3 = [0\ 0\ 1]^T$$

In this case, dim $\mathcal{W}$=rank $\mathbf{T}$=5. $\|\mathbf{T}\mathbf{T}^{+}\mathbf{w}_c - \mathbf{w}_c\| = 1.0$, which implies that $\mathbf{0} \notin$ aff $\mathcal{W}$. We also notice that rank $\mathbf{G}$=6, so dim $\mathcal{W}$ $<$rank $\mathbf{G}$.

Second, four fixels are located collinearly (Fig. 7(*b*)):

$$\mathbf{r}_1 = [0\ \ -40\ 15\sqrt{3}]^T, \quad \mathbf{r}_2 = [0\ \ -15\sqrt{3}/2\ 15\sqrt{3}]^T,$$

$$\mathbf{r}_3 = [0\ 15\sqrt{3}/2\ 15\sqrt{3}]^T, \quad \mathbf{r}_4 = [0\ 40\ 15\sqrt{3}]^T$$

$$\mathbf{n}_1 = [0\ \sqrt{3}/2\ 1/2]^T, \quad \mathbf{n}_2 = [0\ 3/5\ \ -4/5]^T,$$

$$\mathbf{n}_3 = [0\ \ -3/5\ \ -4/5]^T, \quad \mathbf{n}_4 = [0\ \ -\sqrt{3}/2\ 1/2]^T$$

Similarly, dim $\mathcal{W}$=rank $\mathbf{T}$=5. Since $\|\mathbf{T}\mathbf{T}^{+}\mathbf{w}_c - \mathbf{w}_c\| = 0$, $-\mathbf{w}_c \in$ aff $\mathcal{T}$. From Eq. (15), we obtain $p(-\mathbf{w}_c) = 0.1649 < 1$. Thus $\mathbf{0} \in$ ri $\mathcal{W}$. The required CPU time is 68.60 ms.

Third, the fixels are relocated (Fig. 7(*c*))

$$\mathbf{r}_1 = [0\ \ -40\ 15\sqrt{3}]^T, \quad \mathbf{r}_2 = [15\ 0\ 10\sqrt{3}]^T,$$

$$\mathbf{r}_3 = [0\ 40\ 15\sqrt{3}]^T, \quad \mathbf{r}_4 = [-15\ 0\ 10\sqrt{3}]^T$$

$$\mathbf{n}_1 = [0\ \sqrt{3}/2\ 1/2]^T, \quad \mathbf{n}_2 = [-\sqrt{3}/2\ 0\ 1/2]^T,$$

$$\mathbf{n}_3 = [0\ \ -\sqrt{3}/2\ 1/2]^T, \quad \mathbf{n}_4 = [\sqrt{3}/2\ 0\ 1/2]^T$$

Then dim $\mathcal{W}$=rank $\mathbf{T}$=6 and $\|\mathbf{T}\mathbf{T}^{+}\mathbf{w}_c - \mathbf{w}_c\| = 0$. Moreover, we obtain $p(-\mathbf{w}_c) = 1.9245 > 1$ with the CPU time of 64.79 ms. Hence, $\mathbf{0} \in$ aff $\mathcal{W}$ but $\mathbf{0} \notin$ int $\mathcal{W}$.

Finally, the fixel locations are more rational (Fig. 7(*d*)):

$$\mathbf{r}_1 = [0\ \ -30\ 10\sqrt{3}]^T, \quad \mathbf{r}_2 = [0\ 30\ 10\sqrt{3}]^T,$$

$$\mathbf{r}_3 = [15\sqrt{3}/2\ 0\ 15\sqrt{3}]^T, \quad \mathbf{r}_4 = [-15\sqrt{3}/2\ 0\ 15\sqrt{3}]^T$$

$$\mathbf{n}_1 = [0\ \sqrt{3}/2\ 1/2]^T, \quad \mathbf{n}_2 = [0\ \ -\sqrt{3}/2\ 1/2]^T,$$

$$\mathbf{n}_3 = [-3/5\ 0\ \ -4/5]^T, \quad \mathbf{n}_4 = [3/5\ 0\ \ -4/5]^T$$

Then dim $\mathcal{W}$=rank $\mathbf{T}$=6 and $\|\mathbf{T}\mathbf{T}^{+}\mathbf{w}_c - \mathbf{w}_c\| = 0$. With the CPU time of 90.05 ms, we attain $p(-\mathbf{w}_c) = 0.1649 < 1$. Therefore, $\mathbf{0} \in$ int $\mathcal{W}$.

By the proposed force-closure test algorithm, we see that only (d) is force-closure. Neither (a) nor (b) is force-closure, since dim $\mathcal{W} < 6$ in them. If the dimension is ignored, the test for (a) will fall into endless computation and (b) will be mistaken for force-closure, because $\mathbf{0} \in$ int $\mathcal{W}$ is confused with $\mathbf{0} \in$ ri $\mathcal{W}$. (c) fails due to $\mathbf{0} \notin$ int $\mathcal{W}$. The convex hulls $\mathcal{W}$ for (a)–(d) are represented in Figs. 4(*a*)–4(*d*).

Example 2. The object to be grasped is a jar, whose surface consists of a surface of revolution $\mathcal{S}$ and a plane $\mathcal{P}$, as shown in Fig. 8. They can be expressed in parametric form:

$$\mathcal{S}: \begin{cases} r_x = (10\cos(\pi v/30) + 20)\cos\phi \\ r_y = (10\cos(\pi v/30) + 20)\sin\phi \\ r_z = v \end{cases} \qquad \mathcal{P}: \begin{cases} r_x = \rho\cos\theta \\ r_y = \rho\cos\theta \\ r_z = -20 \end{cases}$$

where $-20 \leqslant v \leqslant 40$, $0 \leqslant \phi \leqslant 2\pi$, $0 \leqslant \rho \leqslant 15$, $0 \leqslant \theta \leqslant 2\pi$.

Let us determine an optimal force-closure grasp on the jar with three frictional point contacts. Contacts 1 and 2 are located on $\mathcal{S}$ and contact 3 is located on $\mathcal{P}$. The grasp can be specified by $\mathbf{u} = [v_1\ \phi_1\ v_2\ \phi_2\ \rho\ \theta]$. The initial configuration $\mathbf{u}_0 = [30\ \pi\ 30\ \pi\ 5\ 0]$ and the constraint on $\mathbf{u}$ is given by $[-10\ \varepsilon\ \ -10\ \pi+\varepsilon\ 0\ 0] \leqslant \mathbf{u} \leqslant [30\ \pi-\varepsilon\ 30\ 2\pi-\varepsilon\ 10\ 2\pi]$ where $\varepsilon = 0.01$. The initial grasp is not force-closure since rank $\mathbf{G}$=5, while the

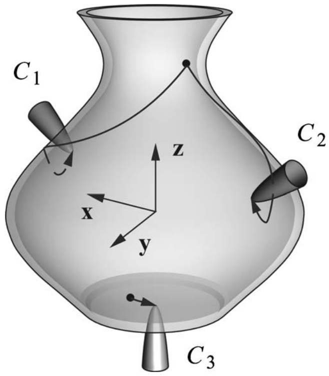

Fig. 8 Towards an optimal grasp on a jar. The dots indicate the initial positions of the fingertips. During the optimization, they trace three curves on the jar surface up to the optimal grasp configuration.

rank of any grasp matrix subject to the constraint is 6. The iterative procedure of Eq. (37) is described in Fig. 9. A force-closure grasp is obtained in five iterations with the CPU time of 12.28 s ($\mathbf{u}_5=[1.9705\ 0.0796\pi\ 1.9457\ 1.0291\pi\ 4.2551\ 0.0813\pi]$, for which $p(-\mathbf{w}_c)=0.4889$). After the 15th iteration, $\mathbf{u}_{15}=[5.9022\ 0.0160\pi\ 5.8499\ 1.0238\pi\ 0.0008\ 0.0990\pi]$ and $p(-\mathbf{w}_c)=0.0230$. Thus we obtain an optimal grasp as depicted in Fig. 8. The CPU time is 38.60 s.

7 Conclusion

(1) The convex hulls of primitive wrenches are classified into four categories by their dimensions and relative positions to the origin of the wrench space (Fig. 4). It is shown that a grasp is force-closure if and only if the convex hull is 6D and the origin is its relative interior point.

(2) We point out the importance of the dimension of the convex hull. Disregarding the dimension, the original ray-shooting approach may make mistakes in force-closure test [4]. To avoid such mistakes, we supplement the condition for the convex hull being 6D; that is, the grasp matrix is full row rank and a certain linear system is consistent.

(3) Whether the origin is a relative interior point of the convex hull is determined by the simplified ray-shooting approach. Its geometric meaning is illustrated clearly in Fig. 6. The consistency of a certain linear system guarantees that the LP formulation in this approach always has an optimal solution.

(4) As a whole, an exact and efficient force-closure test algorithm is developed.

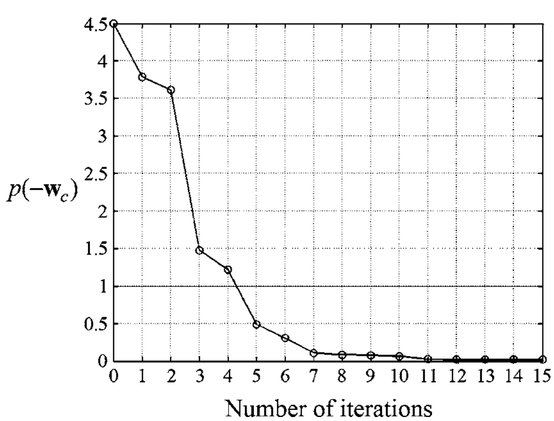

Fig. 9 $p(-\mathbf{w}_c)$ versus the iteration number in Example 2

(5) Our ray-shooting approach presents a the-smaller-the-better performance index. From the ray-shooting viewpoint, it indicates *intuitively* the force-closure safety. Relevant to the inclination angles of contact forces, *physically* it indicates the grasp stability. Using it, we put forward an algorithm for planning force-closure grasps of 3D objects.

(6) The proposed algorithms cover frictionless point contact. By linearizing the constraint at soft finger contact [41], they can be applied to such contact without difficulty.

(7) Needed by this research, we extend theorems in convex analysis for interiors to relative interiors and derive some new results.

Acknowledgment

This work is supported by the National Natural Science Foundation of China under Grant No. 59685004. The authors are very grateful to the reviewers and the editor for their helpful comments and suggestions.

Nomenclature

m = number of contacts
$\mathbf{r}_i$ = position vector of contact i $(i=1,2,\ldots,m)$
$\mathbf{n}_i,\mathbf{o}_i,\mathbf{t}_i$ = unit inward normal and two tangent vectors at contact i, $\mathbf{n}_i=\mathbf{o}_i\times\mathbf{t}_i$
μ = Coulomb friction coefficient at contact
$\mathbf{f}_i$ = contact force at contact i
f_{in}, f_{io}, f_{it} = force components along $\mathbf{n}_i$, $\mathbf{o}_i$, $\mathbf{t}_i$
$\mathbf{G}_i$ = grasp matrix at contact i
$\mathbf{w}_i$ = wrench produced by $\mathbf{f}_i$ on the object
$\mathbf{f}$ = total contact force, $\mathbf{f}=[\mathbf{f}_1^T\mathbf{f}_2^T\cdots\mathbf{f}_m^T]^T\in\mathbb{R}^{3m}$
$\mathbf{G}$ = total grasp matrix, $\mathbf{G}=[\mathbf{G}_1\mathbf{G}_2\cdots\mathbf{G}_m]\in\mathbb{R}^{6\times 3m}$
$\mathbf{w}_{\text{ext}}$ = external wrench on the object
n = number of side edges for linearizing the friction cone
$\mathbf{s}_j$ = the jth edge vector of the polyhedral cone $(j=1,2,\ldots,n)$
$\mathbf{w}_{ij}$ = primitive wrench
$\mathcal{W}$ = convex hull of the primitive wrenches
$\mathbf{w}_c$ = centroid of the primitive wrenches
$\mathcal{T}$ = translate of $\mathcal{W}$ by $-\mathbf{w}_c$
$\mathbf{T}$ = $\mathbf{T}=[\mathbf{w}_{11}-\mathbf{w}_c\cdots\mathbf{w}_{ij}-\mathbf{w}_c\cdots\mathbf{w}_{mn}-\mathbf{w}_c]\in\mathbb{R}^{6\times mn}$
$\mathcal{T}^*$ = polar set of $\mathcal{T}$
p = support function of $\mathcal{T}^*$
$p(-\mathbf{w}_c)$ = value of p with respect to $-\mathbf{w}_c$
$\mathbf{0}$ = origin of a space
$\mathcal{R}$ = ray from $\mathbf{w}_c$ to $\mathbf{0}$
$\text{aff}(\cdot)$ = affine hull of a set
$\dim(\cdot)$ = dimension of a set, i.e., the dimension of the affine hull of the set
$\text{ri}(\cdot)$ = relative interior of a set, i.e., the interior of the set in its affine hull
$\text{cl}(\cdot)$ = closure of a set
$\text{rb}(\cdot)$ = relative boundary of a set
$\text{int}(\cdot)$ = interior of a set
$\text{conv}(\cdot)$ = convex hull of a set

References

[1] Salisbury, J. K., and Roth, B., 1983, "Kinematic and Force Analysis of Articulated Hands," ASME J. Mech., Transm., Autom. Des., **105**(1), pp. 35–41.
[2] Mishra, B., Schwarz, J. T., and Sharir, M., 1987, "On the Existence and Synthesis of Multifingered Positive Grips," Algorithmica, **2**(4), pp. 541–558.
[3] Chen, I.-M., and Burdick, J. W., 1993, "A Qualitative Test for N-Finger Force Closure Grasps on Planar Objects With Applications to Manipulation and Finger Gaits," IEEE International Conference on Robotics and Automation, pp. 814–820.
[4] Liu, Y. H., 1999, "Qualitative Test and Force Optimization of 3-D Frictional Form-Closure Grasps Using Linear Programming," IEEE Trans. Rob. Autom., **15**(1), pp. 163–173.
[5] Zhu, X. Y., Ding, H., and Wang, Y., 2004, "A Numerical Test for the Closure

Properties of 3D Grasps," IEEE Trans. Rob. Autom., **20**(3), pp. 543–549.
[6] Murray, R. M., Li, Z. X., and Sastry, S. S., 1994, *A Mathematical Introduction to Robotic Manipulation*, CRC Press, pp. 223–229.
[7] Zuo, B.-R., and Qian, W.-H., 1998, "A Force-Closure Test for Soft Multi-Fingered Grasps," Sci. China, Ser. E: Technol. Sci., **41**(1), pp. 62–69.
[8] Buss, M., Hashimoto, H., and Moore, J. B., 1996, "Dextrous Hand Grasping Force Optimization," IEEE Trans. Rob. Autom., **12**(3), pp. 406–417.
[9] Han, L., Trinkle, J. C., and Li, Z. X., 2000, "Grasp Analysis as Linear Matrix Inequality Problems," IEEE Trans. Rob. Autom., **16**(6), pp. 663–674.
[10] Bicchi, A., 1995, "On the Closure Properties of Robotic Grasping," Int. J. Robot. Res., **14**(4), pp. 319–334.
[11] Qian, W.-H., Qiao, H., and Tso, S. K., 2001, "Synthesizing Two-Fingered Grippers for Positioning and Identifying Objects," IEEE Trans. Syst. Man Cybern., **31**(4), pp. 602–615.
[12] Xiong, Y. L., Ding, H., and Wang, M. Y., 2002, "Quantitative Analysis of Inner Force Distribution and Load Capacity of Grasps and Fixtures," ASME J. Manuf. Sci. Eng., **124**(2), pp. 444–455.
[13] Zheng, Y., and Qian, W.-H., 2005, "Coping With the Grasping Uncertainties in Force-Closure Analysis," Int. J. Robot. Res., **24**(4), pp. 311–327.
[14] Li, Z. X., and Sastry, S. S., 1988, "Task-Oriented Optimal Grasping by Multifingered Robot Hands," Int. J. Rob. Autom., **4**(1), pp. 32–44.
[15] Kirkpatrick, D., Mishra, B., and Yap, C., 1990, "Quantitative Steinitz's Theorem With Applications to Multi-Fingered Grasping," Proceedings of the 22nd ACM Symposium or Theory of Computing, pp. 341–351.
[16] Ferrari, C., and Canny, J., 1992, "Planning Optimal Grasps," IEEE International Conference on Robotics and Automation, pp. 2290–2295.
[17] Zhu, X. Y., and Wang, J., 2003, "Synthesis of Force-Closure Grasps on 3-D Objects Based on the *Q* Distance," IEEE Trans. Rob. Autom., **19**(4), pp. 669–679.
[18] Varma, V. K., and Tasch, U., 1995, "A New Representation for Robot Grasping Quality Measures," Robotica, **13**(3), pp. 287–295.
[19] Xiong, C. H., and Xiong, Y. L., 1998, "Stability Index and Contact Configuration Planning for Multifingered Grasp," J. Rob. Syst., **15**(4), pp. 183–190.
[20] Salunkhe, B., Mao, W. X., and Tasch, U., 1998, "Optimal Grasping Formulations That Result in High Quality and Robust Configurations," J. Rob. Syst., **15**(12), pp. 713–729.
[21] Nguyen, V.-D., 1988, "Constructing Force-Closure Grasps," Int. J. Robot. Res., **7**(3), pp. 3–16.
[22] Markenscoff, X., and Papadimitriou, C. H., 1989, "Optimum Grip of a Polygon," Int. J. Robot. Res., **8**(2), pp. 17–29.
[23] Park, Y. C., and Starr, G. P., 1992, "Grasp Synthesis of Polygonal Objects Using a Three-Fingered Robot Hand," Int. J. Robot. Res., **11**(3), 163–184.
[24] Tung, C.-P., and Kak, A. C., 1996, "Fast Construction of Force-Closure Grasps," IEEE Trans. Rob. Autom., **12**(4), pp. 615–626.
[25] Chen, I.-M., and Burdick, J. W., 1993, "Finding Antipodal Point Grasps on Irregular Shaped Objects," IEEE Trans. Rob. Autom., **9**(4), pp. 507–512.
[26] Li, J. W., Liu, H., and Cai, H.-G., 2003, "On Computing Three-Finger Force-Closure Grasps of 2-D and 3-D Objects," IEEE Trans. Rob. Autom., **19**(1), pp. 155–161.
[27] Ponce, J., Stam, D., and Faverjon, B., 1993, "On Computing Two-Fingered Force-Closure Grasps of Curved 2D Objects," Int. J. Robot. Res., **12**(3), pp. 263–273.
[28] Ponce, J., and Faverjon, B., 1995, "On Computing Three-Fingered Force-Closure Grasps of Polygonal Objects," IEEE Trans. Rob. Autom., **11**(6), pp. 868–881.
[29] Ponce, J., Sullivan, S., Sudsang, A., Boissonnat, J.-D., and Merlet, J.-P., 1997, "On Computing Four-Fingered Equilibrium and Force-Closure Grasps of Polyhedral Objects," Int. J. Robot. Res., **16**(1), pp. 11–35.
[30] Liu, Y. H., 2000, "Computing *n*-Finger Form-Closure Grasps on Polygonal Objects," Int. J. Robot. Res., **19**(2), pp. 149–158.
[31] Ding, D., Liu, Y. H., and Wang, S. G., 2001, "Computation of 3-D Form-Closure Grasps," IEEE Trans. Rob. Autom., **17**(4), pp. 515–522.
[32] Liu, Y. H., Lam, M. L., and Ding, D., 2004, "A Complete and Efficient Algorithm for Searching 3-D Form-Closure Grasps in the Discrete Domain," IEEE Trans. Rob. Autom., **20**(5), pp. 805–816.
[33] Ding, D., Liu, Y.-H., Wang, Y., and Wang, S. G., 2001, "Automatic Selection of Fixturing Surfaces and Fixturing Points for Polyhedral Workpieces," IEEE Trans. Rob. Autom., **17**(6), pp. 833–841.
[34] Zheng, Y., and Qian, W.-H., 2005, "Simplification of the Ray-Shooting Based Algorithm for 3-D Force-Closure Test," IEEE Trans. Rob. Autom., **21**(3), pp. 470–473.
[35] Howard, W. S., and Kumar, V., 1996, "On the Stability of Grasped Objects," IEEE Trans. Rob. Autom., **12**(6), pp. 904–917.
[36] Lin, Q., Burdick, J. W., and Rimon, E., 2000, "A Stiffness-Based Quality Measure for Compliant Grasps and Fixtures," IEEE Trans. Rob. Autom., **16**(6), pp. 675–688.
[37] Lin, Q., Burdick, J. W., and Rimon, E., 2004, "Computation and Analysis of Natural Compliance in Fixturing and Grasping Arrangements," IEEE Trans. Rob. Autom., **20**(4), pp. 651–667.
[38] Lay, S. R., 1982, *Convex Sets and Their Application*, Wiley, pp. 12, 13, 17, 142, 143.
[39] Steuer, R. E., 1986, *Multiple Criteria Optimization*, Wiley.
[40] Zuo, B.-R., and Qian, W.-H., 1999, "On the Equivalence of Internal and Interaction Forces in Multifingered Grasping," IEEE Trans. Rob. Autom., **15**(5), pp. 934–941.
[41] Zheng, Y., and Qian, W.-H., 2005, "Linearizing the Soft Finger Contact Constraint With Application to Dynamic Force Distribution in Multifingered Grasping," Sci. China, Ser. E: Technol. Sci., **48**(2), pp. 121–130.